78-806

# Wind-Tunnel Blockage Correction for Two-Dimensional Transonic Flow

James A. Blackwell Jr.*
*Lockheed-Georgia Company, Marietta, Ga.*

**An empirical method for correcting two-dimensional transonic flow results for wind-tunnel wall blockage effects has been developed. The empirical method utilizes velocity calculations based on linear theory with free-air boundaries evaluated at vertical positions representative of the wind-tunnel walls and experimental velocity data obtained near the tunnel walls above and below the model. Derivation of the empirical method is presented in detail. Experimental results on 10% and 20% thick supercritical airfoils obtained at transonic speeds and over a wide range of wind-tunnel wall porosities are used to establish the validity of the empirical correction.**

## Nomenclature

$A$ = airfoil cross-sectional area nondimensionalized by the chord squared
$c$ = chord of airfoil, cm (in.)
$C_n$ = section normal-force coefficient
$C_p$ = pressure coefficient
$M$ = freestream Mach number
$\Delta M_B$ = freestream Mach number correction due to solid blockage effects in a wind tunnel
$M_c$ = freestream Mach number corrected for blockage effects
$\bar{M}_E$ = average experimental Mach number evaluated over the model chord at positions above and below the model near the wind-tunnel walls
$\bar{M}_T$ = average theoretical Mach number evaluated over the model chord at a position representative of the wind-tunnel walls
$u/U_\infty$ = perturbation velocity along $X$ axis normalized by freestream velocity
$X,Z$ = Cartesian coordinates with origin at airfoil leading edge and $X$ axis along the airfoil chord, cm (in.)
$\bar{X},\bar{Z}$ = reduced coordinates, Eq. (4)
$\alpha$ = angle of attack, deg
$\beta$ = $\sqrt{1-M^2}$
$\tau$ = wind-tunnel wall porosity (open area/closed area), %
$\mu$ = doublet strength, cm$^2$ (in.$^2$)

*Subscripts*

$c/4$ = airfoil quarter-chord
$D$ = design condition
$\ell$ = lower
$u$ = upper

## Introduction

OVER the years, aerodynamicists have used data from scale-model, wind-tunnel tests to predict the transonic flight characteristics of full-scale aircraft. When this is done, difficulty arises in determining the proper corrections that should be applied to the wind-tunnel data to account for wind-tunnel wall interference. Recent experiments[1] have shown that wall interference on aerodynamic performance at transonic speeds can be very large. Use of conventional subsonic corrections[2] to account for transonic wind-tunnel wall interference effects has been demonstrated in Ref. 1 to be inadequate.

Currently, work on "smart" wind-tunnel walls[3,4] is progressing at a fast pace and appears to offer considerable promise for minimizing wall interference effects. However, even if this approach proves satisfactory, it will still be many years before existing production transonic facilities can be retrofitted with these walls or new tunnels, designed around this concept, constructed.

Sophisticated transonic computational codes which can assess the effects of wind-tunnel wall interference are also under development. Currently, these codes are restricted to viscous two-dimensional flow around airfoils using a small-disturbance formulation which is not adequate for analysis of thick airfoils or inviscid two-dimensional flow using a full-potential formulation.[5,6] Considerable uncertainty still exists as to the proper model for the wind-tunnel walls. Further developments in these codes are expected in the future; however, it will be some time before they are adequately developed and verified to be of general use in determining wall interference effects in conventional transonic wind tunnels.

Until such time as additional facility developments and theoretical advancements are made, it is clear that an interim method for correcting data obtained in conventional transonic wind tunnels for wall interference effects is urgently needed. It is the purpose of this paper to address the development and verification of such an interim approach.

Specific objectives of this work are:

1) Describe an empirical method for correcting transonic flow results for wind tunnel solid model blockage effects.

2) Establish the validity of the empirical blockage correction method using experimental data obtained on 10% and 20% thick supercritical airfoils.

## Empirical Method

### Assumptions

In developing the empirical blockage correction method, two assumptions are made:

1) It is assumed that solid blockage effects at high-subsonic Mach numbers can be adequately represented by a correction to the freestream Mach number. Moreover, this correction is assumed constant over the length of the model.

2)It is assumed that for high-subsonic freestream Mach numbers, the subcritical flowfield surrounding both the

Presented as Paper 78-806 at the AIAA 10th Aerodynamic Testing Conference, San Diego, Calif., April 19-21, 1978; submitted May 22, 1978; revision recieved Oct. 10, 1978. Copyright © American Institute of Aeronautics and Astronautics, Inc., 1978. All rights reserved.

Index categories: Testing, Flight and Ground; Transonic Flow.

*Staff Scientist. Member AIAA.

airfoil and its embedded supercritical flow regions can be adequately described by linear aerodynamics.

The first assumption appears from the outset to be a poor assumption due to the nonlinearity of the transonic flow. However, some evidence, although limited, was presented in Ref. 1 that indicated the gross effects due to solid blockage at transonic conditions were adequately accounted for by a correction to the freestream Mach number. In addition, it is well known that current theoretical airfoil analysis methods (without wall modeling) such as Bauer et al.[7] generally are able to correlate well with wind-tunnel data where wall effects are present. Indeed, it has been observed in Ref. 7 that correlations with airfoil data were further improved for some cases when adjustments were made to the freestream Mach number. It is conjectured here that the gross effects due to solid blockage present in the experimental data shown in Ref. 7 were accounted for by this adjustment to the theoretical freestream Mach number.

The assumption of linear aerodynamics in the subcritical flowfield is good (as indicated in Ref. 8) as long as the calculations are made at some distance from the sonic boundary around the airfoil and the supercritical region in the flowfield is small. As the sonic line is approached, it is obvious that linear theory cannot approximate a nonlinear flowfield. In the following derivation all calculations using linear theory will be made at vertical positions representative of wind-tunnel wall locations. The use of this assumption will improve as the tunnel height-to-chord ratio is increased. The supercritical flowfield requires more space than subsonic flow; therefore, the outer subsonic streamlines around a model are widened outward not only by the model but by the additional displacement due to the supercritical flow. Obviously for conditions where the supercritical flow region is kept small the linear flowfield assumption improves.

To further test the validity of using linear theory to approximate the flowfield in free air at a vertical location representative of wind-tunnel walls, flowfield calculations were made using the aifoil analysis program TSFOIL[5] for a NACA 0010 airfoil at approximately 1.95 chords above the model. These results for a Mach number of 0.83 are shown in Fig. 1. Substantial supercritical flow was present, as evidenced from the pressure distribution shown in Fig. 1. Also included in Fig. 1 is the flowfield predicted using linear aerodynamics [see Eq. (5) in the following section]. As can be seen, the approximation is good. The average deviation in local Mach number in Fig. 1 is less than 0.005.

#### Method Development

Based on the preceding assumptions, the empirical method is postulated as follows: The freestream Mach number correction due to solid blockage can be determined by calculating the average theoretical free-air velocity at a vertical position representative of the wind-tunnel walls using linear theory and subtracting the average experimental velocity measured near the wind-tunnel walls above and below the model to obtain a blockage Mach number correction, denoted $\Delta M_B$. In effect, this approach states that the difference in average velocities measured experimentally near the wind-tunnel walls and what should exist at that location without any walls (free air) represents the blockage Mach number correction. Furthermore, the correction determined in this manner from measurements and calculations near the wall locations is applied uniformly throughout the flowfield.

Based on the preceding postulate, the blockage correction can be expressed mathematically as

$$\Delta M_B = \bar{M}_E - \bar{M}_T \tag{1}$$

The remainder of this section is devoted to the theoretical derivation of the average theoretical Mach number in free air ($\bar{M}_T$) at a position representative of the wind-tunnel walls and an outline of the representative steps necessary to obtain the average experimental Mach number ($\bar{M}_E$) near the wind-tunnel walls.

#### Theoretical Development

The free-air theoretical linear velocity near the wind-tunnel wall is computed by representing the thickness effect of the airfoil with a point doublet located at the airfoil quarter-chord. This arrangement is depicted in Fig. 2. The longitudinal pertubation velocity for a compressible point doublet is given by:

$$\frac{u}{U_\infty} = \frac{\mu}{2\pi\beta}\left\{\frac{(\beta Z)^2 - (X - X_{c/4})^2}{[(X - X_{c/4})^2 + (\beta Z)^2]^2}\right\} \tag{2}$$

The doublet strength $\mu$ is equal to the cross-sectional area of the airfoil. For convenience, the doublet strength will be expressed as

$$\mu = c^2 A \tag{3}$$

where $A$ is the airfoil cross-sectional area nondimensionalized by the chord squared. Defining

$$\bar{X} = \frac{(X - X_{c/4})}{c} \quad \text{and} \quad \bar{Z} = \frac{\beta Z}{c} \tag{4}$$

Eq. (2) becomes

$$\frac{u}{U_\infty} = \frac{A}{2\pi\beta}\left[\frac{\bar{Z}^2 - \bar{X}^2}{(\bar{X}^2 + \bar{Z}^2)^2}\right] \tag{5}$$

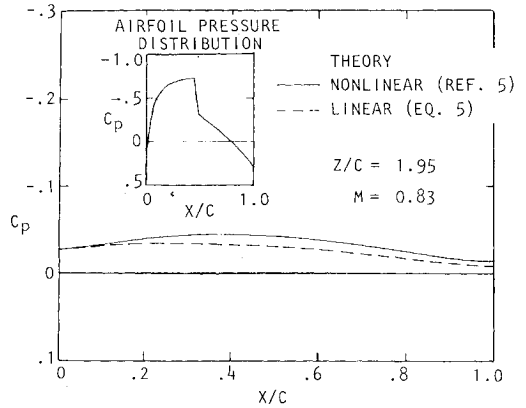


**Fig. 1 Comparison of linear and nonlinear theory in the flowfield for a NACA 0010 airfoil at transonic speeds and $\alpha = 0$ deg.**

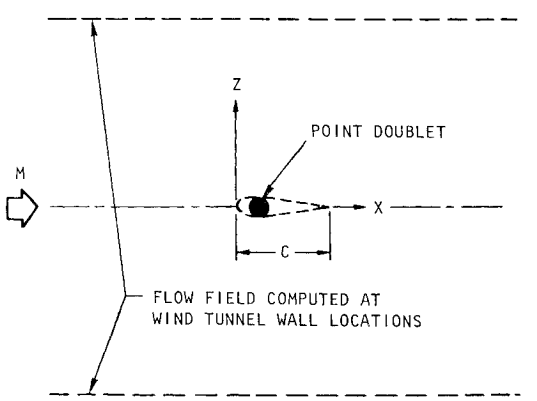


**Fig. 2 Theoretical free-air model.**

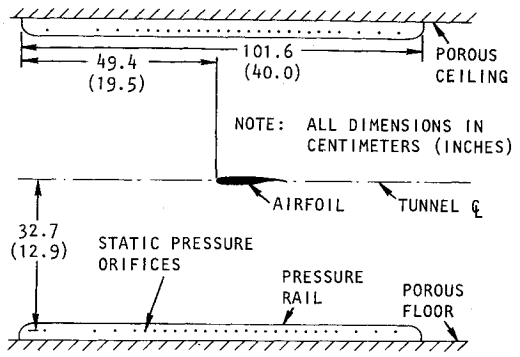


**Fig. 3 Tunnel pressure rail installation.**

Since the blockage correction is assumed to be constant over the length of the airfoil, it is necessary to know only the average pertubation velocity in this region. This is obtained by integrating Eq. (5) over the airfoil chord which yields

$$\frac{\bar{u}}{U_\infty} = \frac{A}{2\pi\beta}\left\{\left[\frac{0.75}{(0.75)^2+\bar{Z}^2}\right]+\left[\frac{0.25}{(0.25)^2+\bar{Z}^2}\right]\right\} \tag{6}$$

The average theoretical Mach number near the wind-tunnel wall over the region influenced by the airfoil can be determined using Eq. (6) and the following isentropic relation relating the velocity perturbation and Mach number

$$\bar{M}_T = \left\{\frac{5+M^2}{1-0.2M^2[(\bar{u}/U_\infty+1)^2-1]}-5\right\}^{1/2} \tag{7}$$

**Experimental Development**

The experimental velocities along the wind-tunnel walls above and below the airfoil model can be measured in solid, slotted, or porous transonic wind tunnels by means of calibrated flush-mounted pressure orifices. Practically, however, this method is often unsatisfactory since it is very difficult to keep foreign matter out of the orifices mounted in the bottom floor and to eliminate disturbances from adjacent holes if the wall is porous.

An alternate means of measuring wall velocities was suggested in Ref. 9 and is shown in Fig. 3. This method uses calibrated pressure rails mounted on the top and bottom wind-tunnel walls. (This method was used in the experimental investigations to be subsequently discussed.)

Irrespective of the method of measurement of the wall Mach number distributions, the average experimental Mach number over the region of the airfoil is computed by:

$$\bar{M}_E = \frac{1}{c}\int_0^c \frac{M_u+M_\ell}{2}\,dx \tag{8}$$

The upper and lower wall distributions are averaged to eliminate the effect of the airfoil lift such that only the effect due to airfoil thickness remains.

## Experimental Verification of Empirical Method

To provide verification of the empirical blockage method, experimental data selected from investigations of 10% and 20% thick supercritical airfoils are used. These data were obtained at transonic speeds over a wide range of porous wall geometries in the Lockheed Compressible Flow Wind Tunnel (CFWT). Both airfoil data and Mach number distributions are available.

A description of the experimental tests will be given first. This will be followed by a discussion of the experimental results. Finally, the empirical blockage correction will be applied to the data and its validity assessed.

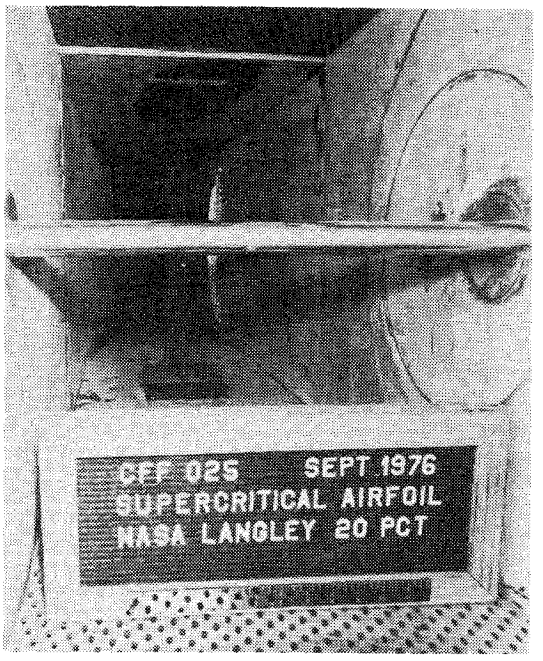


**Fig. 4 Model of 20%-thick supercritical airfoil installed in CFWT.**

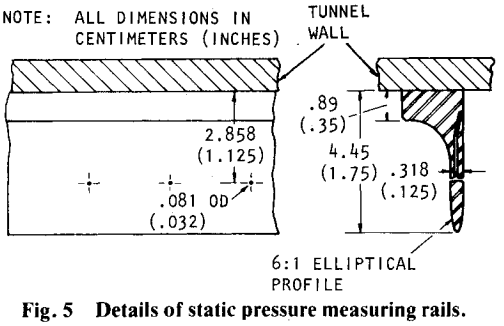


**Fig. 5 Details of static pressure measuring rails.**

**Experimental Tests**

*Test Facility*

The Lockheed-Georgia Compressible Flow Wind Tunnel is a blow-down wind tunnel capable of operating at Mach numbers from 0.2-1.2. The test section with the 20% thick supercritical airfoil model installed is shown in Fig. 4. The test section is 50.8-cm (20-in.) wide × 71.2-cm(28-in.) high × 183-cm (72-in.) long. For two dimensional tests, the test section consists of solid side walls and variable porosity top and bottom walls.

Pressure rails were installed on the tunnel floor and ceiling. These rails were used to make flowfield measurements as close to the tunnel walls as possible without interference from the porous wall. A sketch of the rail design is shown in Fig. 5. This design was patterned after the installation used for similar measurements in Ref. 9.

The variable porosity top and bottom test section walls consist of two adjacent perforated plates with 0.635 cm (0.25 in.) diam holes slanted 60 deg from the vertical. The porosity of the wall may be varied from closed to 10% open by moving the outside shutter plate upstream to misalign the perforations.

*Models*

The supercritical airfoil models have a chord of 17.78 cm (7 in.) and completely span the test section. Surface pressure orifices were installed near the midspan region of the model on the upper and lower surfaces to provide for measurement of the chordwise distribution of pressures.

*Test Techniques*

The airfoil section normal-force and pitching-moment coefficients were computed by integration of the chordwise pressure distributions.

*Test Conditions.*

The data presented for the 10% supercritical airfoil were obtained at a Reynolds number, based on chord, of 7 million. Transition was fixed at the airfoil leading edge (0.05c).

All data for the 20% supercritical airfoil will be presented at a Reynolds number of 11 million. The model was tested without fixing boundary-layer transition, since transition occurred naturally at the airfoil leading edge for this Reynolds number.

The Mach number range of the investigations were 0.6-0.84 and 0.45-0.72 for the 10% and 20% thick supercritical airfoils, respectively. The accuracy of the Mach number for these tests was on the order of ±.003.

*Presentation of Results*

The experimental results presented in this paper will generally be limited to data for the design normal-force coefficient and the design geometric angle of attack which are defined as: $C_{n_D}$ is the airfoil design normal-force coefficient and $\alpha_D$ is the airfoil geometric angle of attack that approximately yields $C_{n_D}$ at the design Mach number.

To better illustrate the pertinent aerodynamic effects, some of the experimental data will be denoted by line symbols rather than point symbols. Also, the force data variations will be presented in incremental form with results for a wind-tunnel wall porosity of 4% used as a datum.

**Experimental Results**

The results for the 20% supercritical airfoil will be presented first since it represents the most severe test of the empirical blockage method.

*Twenty Percent Supercritical Airfoil*

In order to evaluate Eq. (8), the Mach number distributions near the wall are required. Typical Mach number distributions near the top and bottom walls for the 20% supercritical airfoil at its design normal-force coefficient and Mach number (0.70) are presented in Fig. 6 for wind-tunnel wall porosities of 2, 4, 6, and 8%. The substantial influence of porosity is obvious.

Data, such as those in Fig. 6, have been integrated according to Eq. (8) to yield the average experimental Mach number ($\bar{M}_E$) at the wall over the region of the model. These results then have been combined with the average theoretical Mach number ($\bar{M}_T$) at the wall over the region of the model, as calculated from Eq.(7), to yield the empirical blockage Mach number correction ($\Delta M_B$). Typical results from this process are shown in Fig. 7 at wall porosities of 2% and 4% for a series of model angles of attack. As can be seen, the blockage correction is invariant with normal-force coefficient. This is also true for the other porosities investigated (6% and 8%).

Using a mean of the data for each freestream Mach number in Fig. 7 and doing likewise for similar data at porosities of 6% and 8%, the blockage corrections can be summarized in Fig. 8 independent of normal-force coefficient. As can be seen, the results indicate the blockage correction to be zero near a wall porosity of 4%. Also the correction is largest as a closed wall is approached, as would be expected. The data in Fig. 8 are presented in an alternate manner in Fig. 9. As indicated in this figure, the blockage correction increases rapidly with Mach number.

Airfoil pressure distributions for the 20% supercritical airfoil at a Mach number of 0.70, and the design angle of attack are presented in Fig. 10. As can be seen, the differences in the data over the porosity range of 2-8% are substantial. Some of the differences are eliminated when the data are

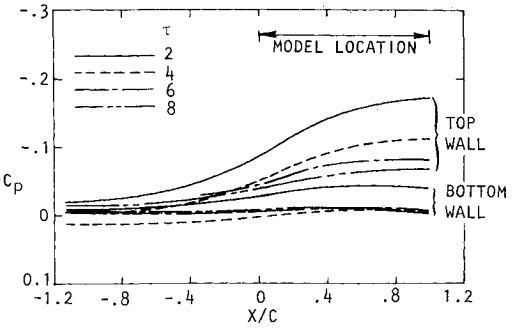


**Fig. 6 Variation of wall pressure distribution with porosity at design normal-force coefficient for 20% supercritical airfoil, $M = 0.70$.**

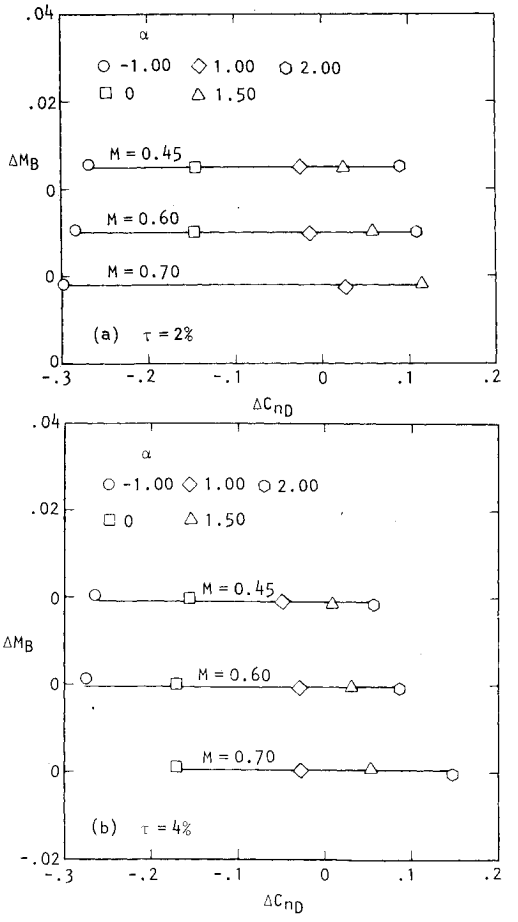


**Fig. 7 Variation of blockage Mach number correction with normal force coefficient for 20% supercritical airfoil.**

compared at a constant normal-force coefficient (Fig. 11) since lift interference effects are neutralized. The remaining effects can be attributed to solid blockage interference.

Using the blockage corrections to Mach number shown in Fig. 9, experimental data were obtained for the 20% supercritical airfoil at freestream Mach numbers equal to $M - \Delta M_B$ for each of the four wall porosities (2, 4, 6, and 8%). Application of the blockage corrections to these data should then result in the same corrected freestream Mach number ($M_c$) for each wall porosity. If these data collapse at a constant normal-force coefficient, then it can be concluded that the empirical method has provided corrections of the proper magnitude.

Data obtained in the preceding manner is presented in Fig. 12. The differences in airfoil pressure distribution relative to those shown in Fig. 11 are considerably smaller. In particular, only small differences occur in the pressure distributions for

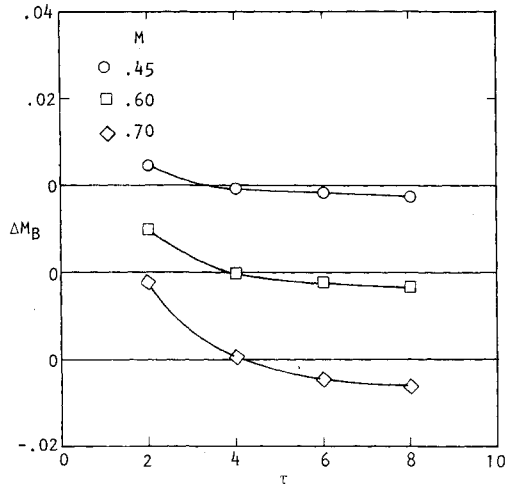


**Fig. 8 Variation of blockage Mach number correction with porosity for 20% supercritical airfoil.**

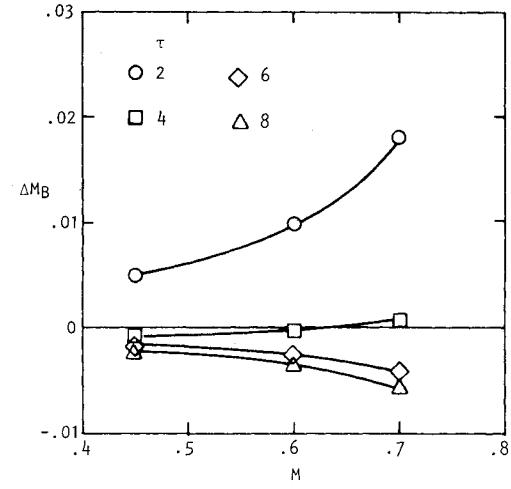


**Fig. 9 Variation of blockage Mach number correction with nominal freestream Mach number for 20% supercritical airfoil.**

wall porosities of 4, 6, and 8%. The pressure data for 2% porosity is in substantially better agreement with the other porosity data than was the case when no corrections were applied in Fig. 11. However, some discrepancies still remain. Part of this difference may be explained by the 2% data being obtained at a slightly lower normal-force coefficient than the other results.

From the comparison of the pressure distributions for the various wall porosities (Fig. 12), it generally can be concluded that the corrections provided by the emprical blockage method do indeed provide Mach number corrections of the right order of magnitude to collapse the data obtained at various wall conditions. Also, it appears that a correction to freestream Mach number is sufficient to account for the gross solid blockage effects on the data.

*Ten Percent Supercritical Airfoil*

Typical Mach number distributions near the top and bottom walls for the 10% supercritical airfoil at its design normal-force coefficient and Mach number (0.80) are presented in Fig. 13 for wind-tunnel wall porosities of 2, 4, and 6%. As with the 20% supercritical airfoil, the substantial influence of porosity is obvious.

Data, such as those shown in Fig. 13, have been integrated according to Eq. (8) and combined with the theoretical results of Eq. (7) to yield the empirical blockage Mach number corrections for the 10% supercritical airfoil. The results are shown in Fig. 14.

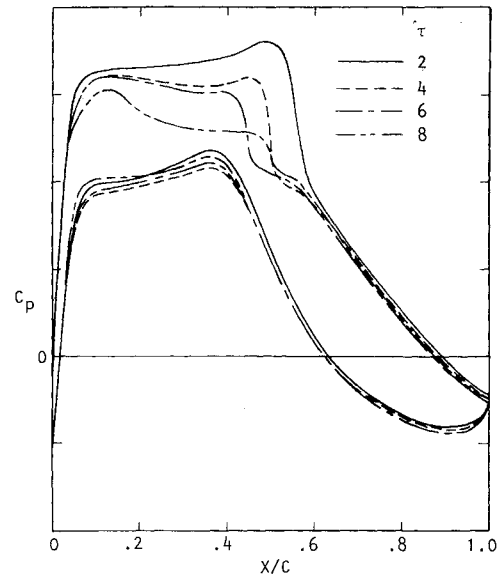


**Fig. 10 Variation of airfoil pressure distribution with porosity at design angle of attack for 20% supercritical airfoil, $M = 0.70$.**

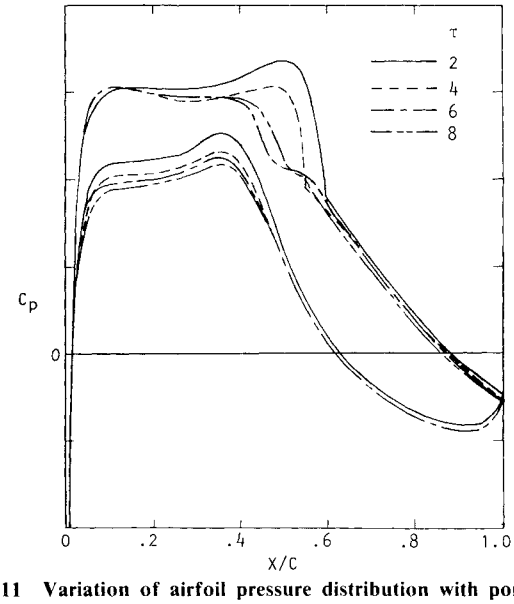


**Fig. 11 Variation of airfoil pressure distribution with porosity at design normal-force coefficient for 20% supercritical airfoil, $M = 0.705$.**

Airfoil pressure distributions for the 10% supercritical airfoil at a Mach number of 0.80 and the design angle of attack are presented in Fig. 15. The effect of changing wall porosity as shown in this figure is substantial. The shock travel is approximately 30% chord. The variation in pressure distributions shown in Fig. 15 is reduced by comparing the data at constant normal-force coefficient. This comparison is presented in Fig. 16. However, considerable differences still remain that can be attributed to solid blockage wall interference.

Experimental data were obtained for the 10% supercritical airfoil at freestream Mach numbers equal to $M - \Delta M_B$ where the blockage correction was determined from Fig. 14. These data are shown for a corrected freestream Mach number of 0.8 in Fig. 17 for wall porosities of 2 and 4%. The differences in pressure distribution relative to that in Fig. 16 are substantially smaller. In general, it can be said the agreement in Fig. 17, considering the small difference in normal-force coefficient, is good.

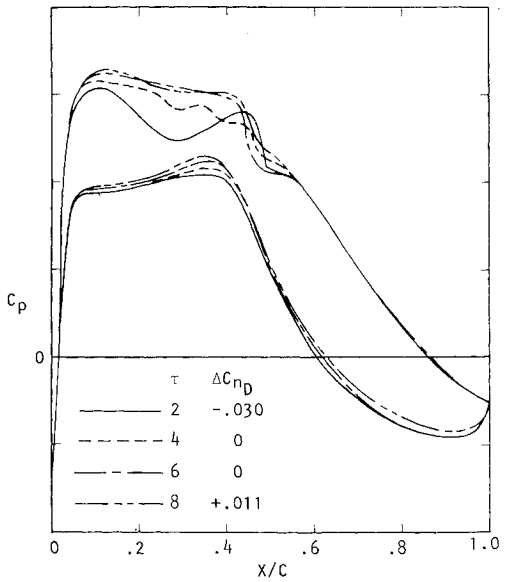


**Fig. 12 Variation of airfoil pressure distribution with porosity at design normal-force coefficient for 20% supercritical airfoil, $M_c = 0.700$.**

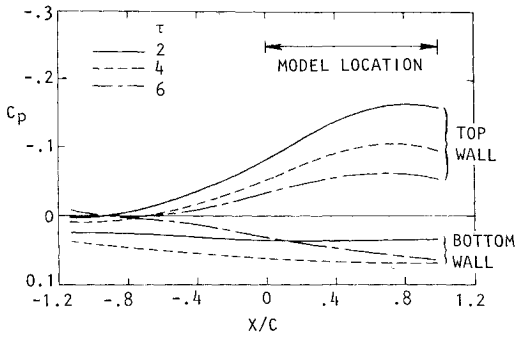


**Fig. 13 Variation of wall pressure distributions with porosity at design normal-force coefficient for 10% supercritical airfoil, $M = 0.80$.**

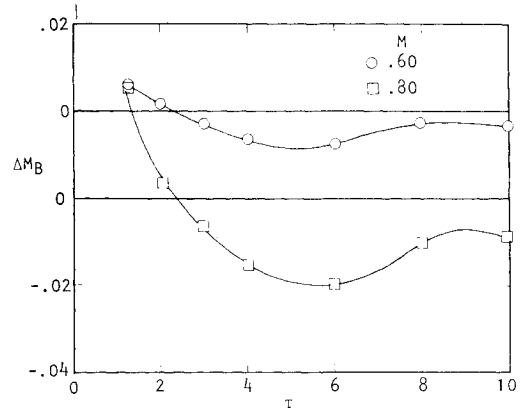


**Fig. 14 Variation of blockage Mach number correction with porosity for 10% supercritical airfoil.**

As with the 20% supercritical airfoil, it generally can be concluded that the empirical blockage method does provide corrections of the right order of magnitude to collapse the data obtained at various wall conditions.

*Summary*

Although the data presented to verify the empirical blockage method are limited, it does appear that the method provides blockage corrections of the right order of magnitude to collapse data obtained for various wall conditions. It can only be inferred that the corrected airfoil wind-tunnel data approximate free-air results since the average flowfield characteristics near the wall are the same. Also it can be concluded that a correction to freestream Mach number is sufficient to account for the gross solid blockage effects on the data.

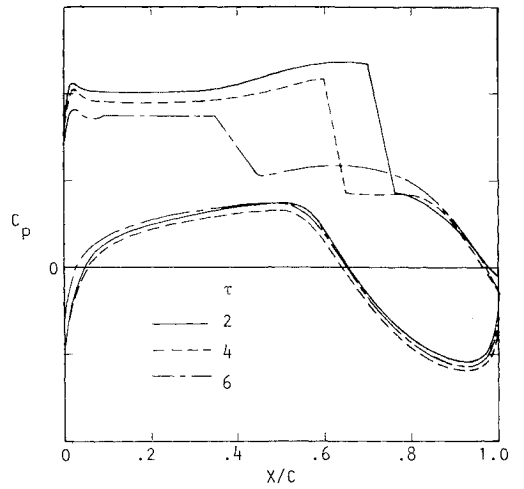


**Fig. 15 Variation of airfoil pressure distribution with porosity at design angle of attack for 10% supercritical airfoil, $M = 0.80$.**

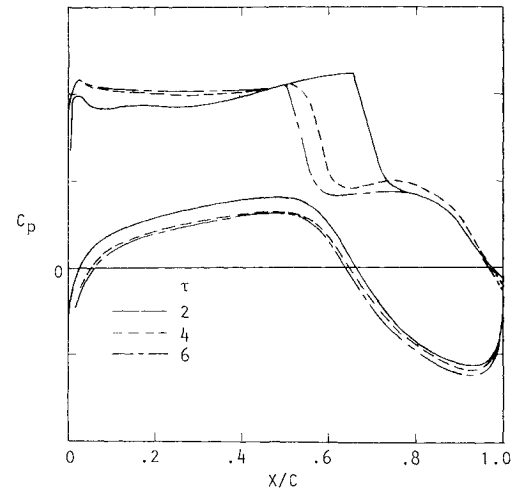


**Fig. 16 Variation of airfoil pressure distribution with porosity at design normal-force coefficient for 10% supercritical airfoil, $M = 0.80$.**

## Comparison of Correction Methods

Since subcritical methods have been used in the past to account for solid blockage effects at subsonic and transonic speeds, it is of interest to compare the corrections predicted by these methods with those of the empirical approach. Two subcritical methods were considered. The first is the conventional AGARD subcritical wall interference correction method of Ref. 2. This approach assumes the wall resistance factors for a porous wall to be the same on the top and bottom wind-tunnel walls. Values of the resistance factor are determined empirically. Those used in the present comparison were taken from Ref. 10.

A second method has been developed at NAE[9] which allows a differential wall resistance factor between the top and bottom walls. This method is based on the observation that the individual tunnel walls may have different resistances to the flow depending on whether they are experiencing inflow

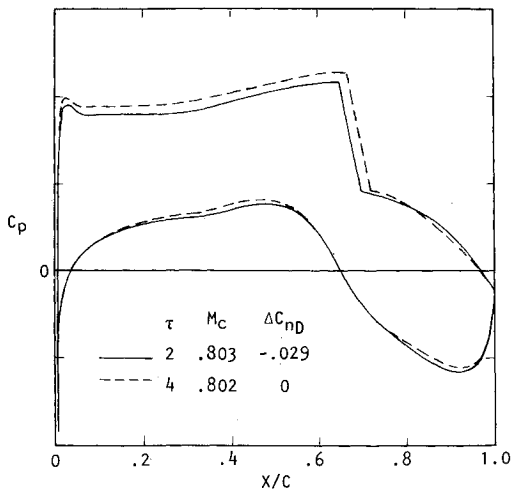


**Fig. 17 Variation of airfoil pressure distribution with porosity at design normal-force coefficient for 10% supercritical airfoil, $M_c = 0.80$.**

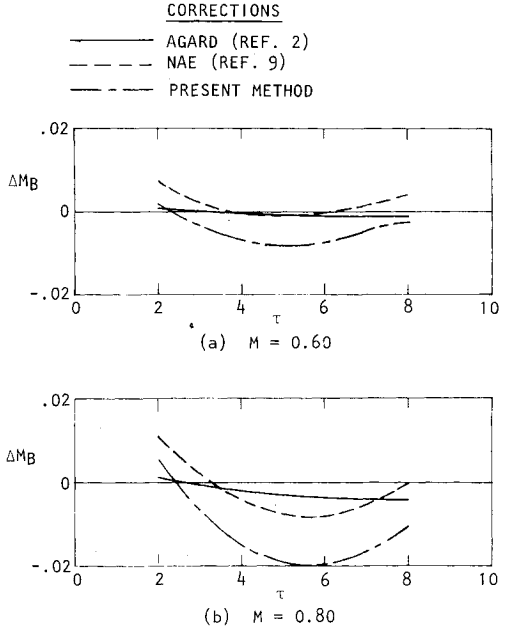


**Fig. 18 Wind-tunnel blockage corrections at design normal-force coefficient for 10% supercritical airfoil.**

from the plenum chamber into the test section or outflow from the tunnel test section into the plenum chamber. The resistance factors for each wall are determined by matching the theoretical wall (top and bottom) pressure distributions with the experimental data.

The blockage corrections to Mach number as calculated from the two subcritical methods are compared with the results from the present empirical approach in Figs. 18 and 19 for the 10% and 20% supercritical airfoils, respectively.

In Figs. 18 and 19, the AGARD corrections can be seen to be substantially smaller in magnitude than the other methods. From the data presented herein, it has been shown that corrections of substantially greater magnitude than that predicted by the AGARD method are needed to correlate the experimental data for the various wall porosities. Clearly, this method is inadequate to predict blockage corrections at transonic speeds.

The NAE wall-matching method yields results that are approximately the same order of magnitude as produced by the empirical approach; however, the NAE corrections are

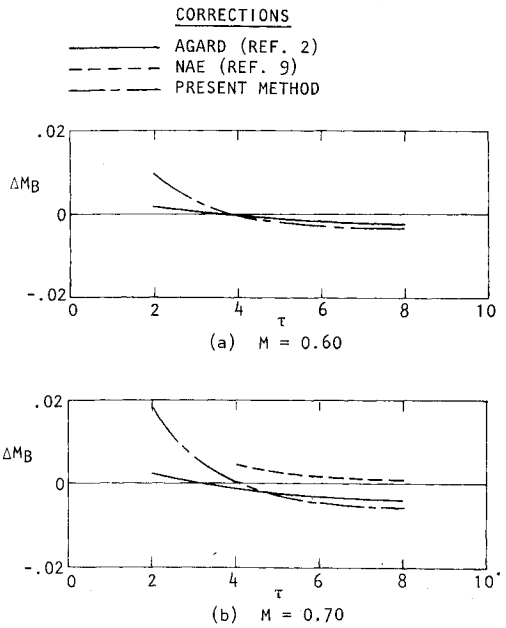


**Fig. 19 Wind-tunnel blockage corrections at design normal-force coefficient for 20% supercritical airfoil.**

generally displaced in the positive direction. Consequently, the porosity for zero blockage, as indicated by the NAE method, generally occurs at a higher value of porosity than that given by the empirical approach. In particular for the 20% supercritical airfoil at $M = 0.70$ (Fig. 19), no value of zero blockage Mach number was found over the porosity range investigated.

No solution could be obtained from the NAE method for a porosity of 2% and Mach number of 0.70 for the 20% supercritical airfoil. This was due to the failure of the linear theory to predict flowfield velocities higher than the freestream value on the lower wall (see Fig. 6) for any combination of wall resistance factors.

## Concluding Remarks

An empirical method for correcting two-dimensional transonic flow results for wind-tunnel blockage effects has been developed. The empirical method utilizes velocity calculations based on linear theory and experimental velocity data obtained near the wind-tunnel walls.

Experimental results on 10% and 20% thick supercritical airfoils obtained at transonic speeds over a wide range of wind-tunnel wall porosities have been used to establish the validity of the empirical blockage correction. It can be concluded from this validation process that for the range of airfoils and Mach numbers investigated, a simple correction to the freestream Mach number is sufficient to account for the gross solid blockage effects.

The experimental verification also indicated that the empirical method does provide blockage corrections to the freestream Mach numbers that are of the right order of magnitude needed to collapse the experimental airfoil data obtained for various wind-tunnel wall conditions. It only can be inferred at this time until additional experimental studies are accomplished that the corrected airfoil wind-tunnel data approximates free-air results. This inference is based on the average flowfield characteristics being the same for the experimental wind-tunnel data near the wall and the theoretical free-air results at vertical positions representative of the wall.

## References

[1] Blackwell, Jr., J. A., and Pounds, G. A., "Wind-Tunnel Wall Interference Effects on a Supercritical Airfoil at Transonic Speeds," *Journal of Aircraft*, Vol. 14, Oct. 1977, pp. 929-935.

[2]Garner, H. C., Rogers, E. W. E., Acum, W. E. A., and Maskell, E. C., "Subsonic Wind Tunnel Wall Corrections," AGARDograph 109, 1966.

[3]Sears, W. R., Vidal, R. J., Erickson, J. C., and Ritter, A., "Interference-Free Wind Tunnel Flows by Adaptive-Wall Technology," ICAS Paper 76-02, Oct. 1976.

[4]Goodyer, M. J., "The Self Streamlining Wind Tunnel," NASA TM X-72699, Aug. 1975.

[5]Murman, E. M., Bailey, F. R., and Johnson, M. L., "TSFOIL-A Computer Code for Two-Dimensional Transonic Calculations, Including Wind-Tunnel Wall Effects and Wave-Drag Evaluation," NASA SP-347, 1975.

[6]Kacprzynski, J. J., "Transonic Flowfield Past 2-D Airfoils Between Porous Wind Tunnel Walls with Nonlinear Characteristics, AIAA Paper 75-81, *AIAA Journal*, April 1976, pp. 533-535.

[7]Bauer, F., Garabedian, P., Korn, D., and Jameson, A., "Supercritical Wing Sections II," *Lecture Notes in Economics and Mathematical Systems 108*, Springer-Verlag, 1975.

[8]Göthert, B., and Kawalki, K. H., "The Calculation of Compressible Flows with Local Regions of Supersonic Velocity," NACA TM No. 1114, March 1947.

[9]Mokry, M., Peake, D. J., and Bowker, A. J., "Wall Interference on Two-Dimensional Supercritical Airfoils, Using Wall Pressure Measurements to Determine the Porosity Factors for Tunnel Floor and Ceiling," NAE LR-575, 1974.

[10]Pounds, G. A., "An Initial Two-Dimensional Wall Interference Investigation in a Transonic Wind Tunnel with Variable Porosity Test Section Walls," AIAA Paper 72-1011, Palo Alto, Calif., Sept. 13-15, 1972.

*From the AIAA Progress in Astronautics and Aeronautics Series*

**AERODYNAMICS OF BASE COMBUSTION—v. 40**

*Edited by S.N.B. Murthy and J.R. Osborn, Purdue University, A. W. Barrows and J. R. Ward, Ballistics Research Laboratories*

It is generally the objective of the designer of a moving vehicle to reduce the base drag—that is, to raise the base pressure to a value as close as possible to the freestream pressure. The most direct and obvious method of achieving this is to shape the body appropriately—for example, through boattailing or by introducing attachments. However, it is not feasible in all cases to make such geometrical changes, and then one may consider the possibility of injecting a fluid into the base region to raise the base pressure. This book is especially devoted to a study of the various aspects of base flow control through injection and combustion in the base region.

The determination of an optimal scheme of injection and combustion for reducing base drag requires an examination of the total flowfield, including the effects of Reynolds number and Mach number, and requires also a knowledge of the burning characteristics of the fuels that may be used for this purpose. The location of injection is also an important parameter, especially when there is combustion. There is engineering interest both in injection through the base and injection upstream of the base corner. Combustion upstream of the base corner is commonly referred to as external combustion. This book deals with both base and external combustion under small and large injection conditions.

The problem of base pressure control through the use of a properly placed combustion source requires background knowledge of both the fluid mechanics of wakes and base flows and the combustion characteristics of high-energy fuels such as powdered metals. The first paper in this volume is an extensive review of the fluid-mechanical literature on wakes and base flows, which may serve as a guide to the reader in his study of this aspect of the base pressure control problem.

*522 pp., 6×9, illus. $19.00 Mem. $35.00 List*

TO ORDER WRITE: Publications Dept., AIAA, 1290 Avenue of the Americas, New York, N. Y. 10019